



HAL
open science

Revisiting horizontal connectivity rules in V1: from like-to-like towards like-to-all

Frédéric Chavane, Laurent Perrinet, James Rankin

► **To cite this version:**

Frédéric Chavane, Laurent Perrinet, James Rankin. Revisiting horizontal connectivity rules in V1: from like-to-like towards like-to-all. *Brain Structure and Function*, 2022, 10.1007/s00429-022-02455-4. hal-03572602

HAL Id: hal-03572602

<https://hal.science/hal-03572602>

Submitted on 15 Mar 2022

HAL is a multi-disciplinary open access archive for the deposit and dissemination of scientific research documents, whether they are published or not. The documents may come from teaching and research institutions in France or abroad, or from public or private research centers.

L'archive ouverte pluridisciplinaire **HAL**, est destinée au dépôt et à la diffusion de documents scientifiques de niveau recherche, publiés ou non, émanant des établissements d'enseignement et de recherche français ou étrangers, des laboratoires publics ou privés.

1 Revisiting horizontal connectivity rules in V1: from like-to-like towards 2 like-to-all

3 Chavane F^{1*}, Perrinet L¹, Rankin J²,

4 ¹ Institut de Neurosciences de la Timone (INT), CNRS and Aix-Marseille Université, UMR 7289,
5 Campus Santé Timone, 27 boulevard Jean Moulin, Marseille 13005, France

6 ² Department of Mathematics, College of Engineering, Mathematics & Physical Sciences,
7 University of Exeter, Exeter EX4 4QJ, United Kingdom;

8 * correspondence to FC, frederic.chavane@univ-amu.fr

9 Abstract

10

11 Horizontal connections in the primary visual cortex of carnivores, ungulates and primates
12 organise on a near-regular lattice. Given the similar length-scale for the regularity found in
13 cortical orientation maps, the currently accepted theoretical standpoint is that these maps are
14 underpinned by a like-to-like connectivity rule: horizontal axons connect preferentially to
15 neurons with similar preferred orientation. However, there is reason to doubt the rule's
16 explanatory power, since a growing number of quantitative studies show that the like-to-like
17 connectivity preference and bias are mostly observed at short-range scale, are highly variable
18 on a neuron-to-neuron level and also depend on the origin of the presynaptic neuron. Despite
19 the wide availability of published data to this effect, the accepted model of visual processing has
20 never been revised. We review three lines of independent evidence supporting a much-needed
21 revision of the like-to-like connectivity rule, ranging from anatomy to population functional
22 measures, to computational models and theoretical approaches. We advocate an alternative,
23 distance-dependent connectivity rule that is consistent with new structural and functional
24 evidence: **from like-to-like bias at short horizontal distance to like-to-all at long horizontal**
25 **distance**. This generic rule accounts for the observed high heterogeneity in interactions
26 between the orientation and retinotopic domains, that we argue is necessary to process non-
27 trivial stimuli in a task-dependent manner.

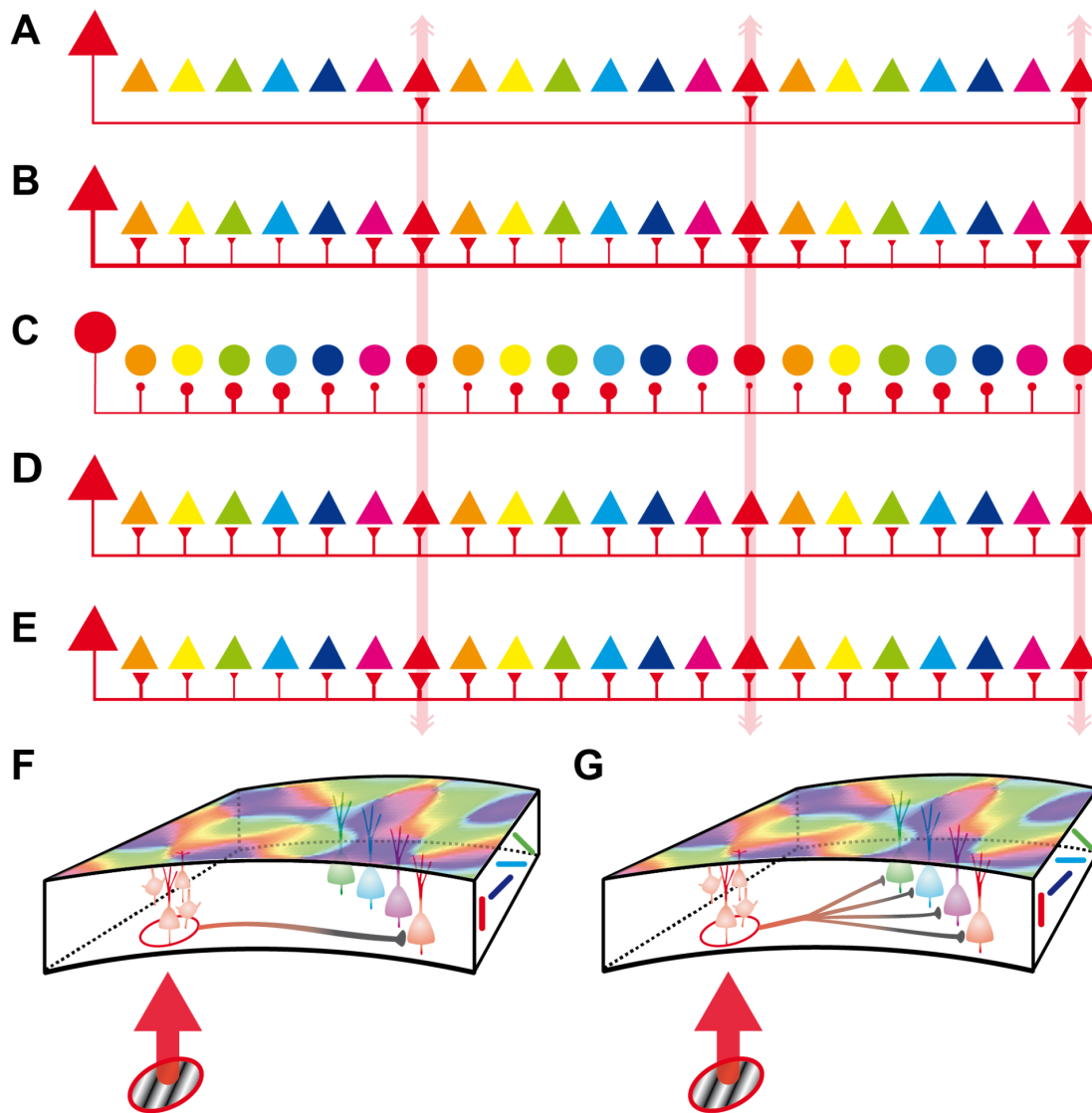
28 INTRODUCTION

29 Retinotopy and orientation are two of the main features processed and topographically
30 organized into maps in primary visual cortex (V1) of carnivores, ungulates and primates.
31 Anatomical connections between neurons separated on the cortical sheet, through the so-called
32 *intrinsic, intra-cortical or horizontal* axons have a crucial theoretical importance for
33 understanding the computational operations that V1 can perform. Indeed, these axons connect
34 different points in the retinotopic and orientation maps and thereby generate a set of possible
35 topological interactions within a multidimensional representation of space, orientation and time.
36 It is therefore critical to characterize structural horizontal interactions in order to understand their
37 functional relevance. The vast majority of presynaptic contacts in cortex originate from neurons
38 located in the same area as the postsynaptic target (>80% in macaque V1, (Markov et al. 2011),
39 thus forming an intra-cortical network. In the primary visual cortex, the feedforward
40 thalamocortical inputs drive the cortical network, which in turn strongly shapes the evoked
41 response through major excitatory and inhibitory recurrent circuits within the column (Douglas et
42 al. 1991), a canonical circuit that constitutes nearly $\frac{2}{3}$ of intra-cortical connectivity (Markov et al
43 2011). The rest of the intra-cortical network connects neurons in adjacent columns separated
44 laterally over distances up to several millimeters, the so-called horizontal network. Early
45 anatomical observations reported that the horizontal connectivity of carnivores, ungulates and
46 primates is spatially distributed into regular clusters (Fig. 1A, (Braitenberg 1962; Fisker et al.
47 1975; Creutzfeldt et al. 1977; Gilbert and Wiesel 1979; Rockland et al. 1982) forming a radially
48 projecting pattern that resembles a daisy's petals (Douglas and Martin 2004). Since orientation
49 maps are also regular with comparable spatial frequency, the currently accepted theoretical
50 standpoint is that these maps are underpinned by a **like-to-like connectivity rule**: cortical
51 columns are connected by horizontal connections only if they share similar orientation
52 preference (Fig. 1A), an hypothesis originally put forward by Mitchison & Crick (Mitchison and
53 Crick 1982). Correlative studies, comparing bouton labelling with autoradiography, or with
54 optical imaging maps, qualitatively supported the like-to-like rule (Gilbert and Wiesel 1989).
55 Later quantitative anatomical combined with optical imaging studies confirmed the existence of
56 an orientation preference bias (Fig. 1B, in the range of 1.5-2 times greater than chance, [Bosking](#)
57 [et al. 1997](#), [Kisvárdy 1997](#); [Schmidt et al. 1997](#); [Malach et al., 1993](#), [Rocheffort et al., 2009](#)),
58 with high cell-to-cell variability. Probably due to its simplicity and its elegant topological
59 implications, the highlighted iso-orientation biases have led to a general acceptance of the
60 hypothesis of a simplified and unique like-to-like connectivity. One consequence is that
61 theoretical and computational models have implemented it as a strict rule, not as a bias (e.g.
62 (Bressloff et al. 2001; Raizada and Grossberg 2003; Rangan et al. 2005; Sarti et al. 2008; Baker
63 and Cowan 2009; Kaschube et al 2010; Rubin et al. 2015; Carroll and Bressloff 2016).
64 However, we believe such an over-simplified schema may impair the development of our
65 theoretical understanding of the primary visual cortex function.

66

67 Actually, there are reasons to doubt the explanatory power of a global and strict like-to-like
68 connectivity rule. First, a growing number of quantitative studies show that there is a wide
69 variety of connectivity biases (like-to-like bias, no bias, like-to-unlike bias) depending on cell
70 type (Fig. 1C, excitatory vs inhibitory neurons, see [Kisvárdy et al. 1994](#); [Buzás et al. 2001](#)),

71 layer origin (Fig. 1D, no bias in layer 4 or layer 6, see Yousef et al. 1999; Karube and Kisvarday
72 2010; Karube et al. 2017), and position in the orientation map (Yousef et al. 2001, iso-
73 orientation domain vs pinwheels). Second, the effect is mostly observed at short-range where
74 most of the connectivity arises (<1-1.5mm), but connections can connect neurons over
75 distances of a few millimeters. The rare analyses over larger cortical distances (more difficult
76 because far fewer boutons are present) showed a global tendency for the iso-orientation bias to
77 reduce with distance (Fig. 1E) due to wider selectivity or deviation from the iso-orientation bias,
78 as observed in Buzás et al. (2006, fig8C), Kisvarday et al (1997, Fig9 - area 17) and Bosking et
79 al (1997, Fig 5); however, see a counter example for area 18 in Kisvarday et al (1997, Fig10 –
80 area 18). As a consequence, the effective functional selectivity of horizontal axons beyond the
81 short-range distance is not very clear. Lastly, the functional impact of the structural organisation,
82 as described by anatomy, is far from being trivial to predict. Indeed, any visual stimulation will
83 activate a neuronal mass encompassing all layers, both excitatory and inhibitory neurons and at
84 least a full hypercolumn composed of pinwheels and iso-orientation domains (see Fig1D in
85 Chavane et al 2011). Furthermore, not only neurons with preferred orientation matching the
86 orientation of the stimulus will be significantly activated, but a distribution of neurons with say,
87 +/-15 deg around the stimulus orientation. The intra-cortical horizontal network triggered by this
88 functionally activated neuronal mass will forcibly contact a diversity of orientation tuned neurons
89 (ranging from an iso-orientation, Fig. 1F, to an omni-orientation interaction, Fig. 1G) with an
90 overall net effect beyond short-range distance that is particularly difficult to predict.



91

92 **Fig. 1: Illustration of different connectivity rules from literature and possible outcomes for**
 93 **functional activation.** In A-E the local neuron (large on left) connects to neighbours in a radially
 94 approximated schema spanning outwards over three hypercolumns (where the same preference is
 95 encountered, as indicated by the vertical arrows). Colors indicate the orientation preference of neurons.
 96 **(A)** Strict like-to-like connectivity (extends to long distances). **(B)** Modulated like-to-like bias (extends to
 97 long distances). **(C)** Like-to-unlike bias as exhibited by inhibitory interneuron. **(D)** Like-to-all as exhibited
 98 by neurons in layer 4 and 6. **E:** Like-to-like bias that reduces with distance resulting in like-to-all at
 99 distances beyond adjacent hypercolumns. **(F-G)** Two extremes hypothesis for the net outcome of
 100 functionally driven connectivity rule at long-range distance. In response to a local oriented stimulus, all
 101 neurons that have a receptive field in overlap with the stimulus will be activated, for excitatory and
 102 inhibitory neurons, different lamina and positions in the orientation map. Such functional activation can
 103 lead either to a strict iso-orientation activation of neighboring neurons through the horizontal network (like-
 104 to-like rule, F) or omni-orientation activation (like-to-all rule, G).

105 In this review, we present a body of recent evidence from anatomy, physiology and
106 computational modeling, leading to the conclusion that horizontal interactions do not forcibly
107 conform with a like-to-like orientation preference. In the last decade, structural (Hunt et al. 2011;
108 Martin et al. 2014, see Kisvarday 2016 for review), and functional (Chavane et al. 2011; Huang
109 et al. 2014) studies have shown that the rule is not valid for long-distance connections. Chavane
110 et al (2011) proposed revisiting the connectivity rule as a function of horizontal distance: from
111 like-to-like at short distance towards like-to-all and long distances (Fig. 1E; see discussion in
112 (Alonso and Kremkow 2014a, b). In their computational modelling study, (Rankin and Chavane
113 2017) show that this behavior is in fact to be expected based on the anatomical observations
114 made by Buzas et al (2006). The functional implications of such evidence is further discussed in
115 the framework of natural scenes analysis (Perrinet and Bednar 2015; Boutin et al. 2021). In light
116 of converging evidence from a range of approaches, this review argues for a timely, in-depth
117 revision of V1 horizontal connectivity rules. Revisiting this textbook mindset is an important
118 prerequisite to better understand the relationship between structure and function in the visual
119 cortex.

120 NEW PHYSIOLOGICAL EVIDENCE

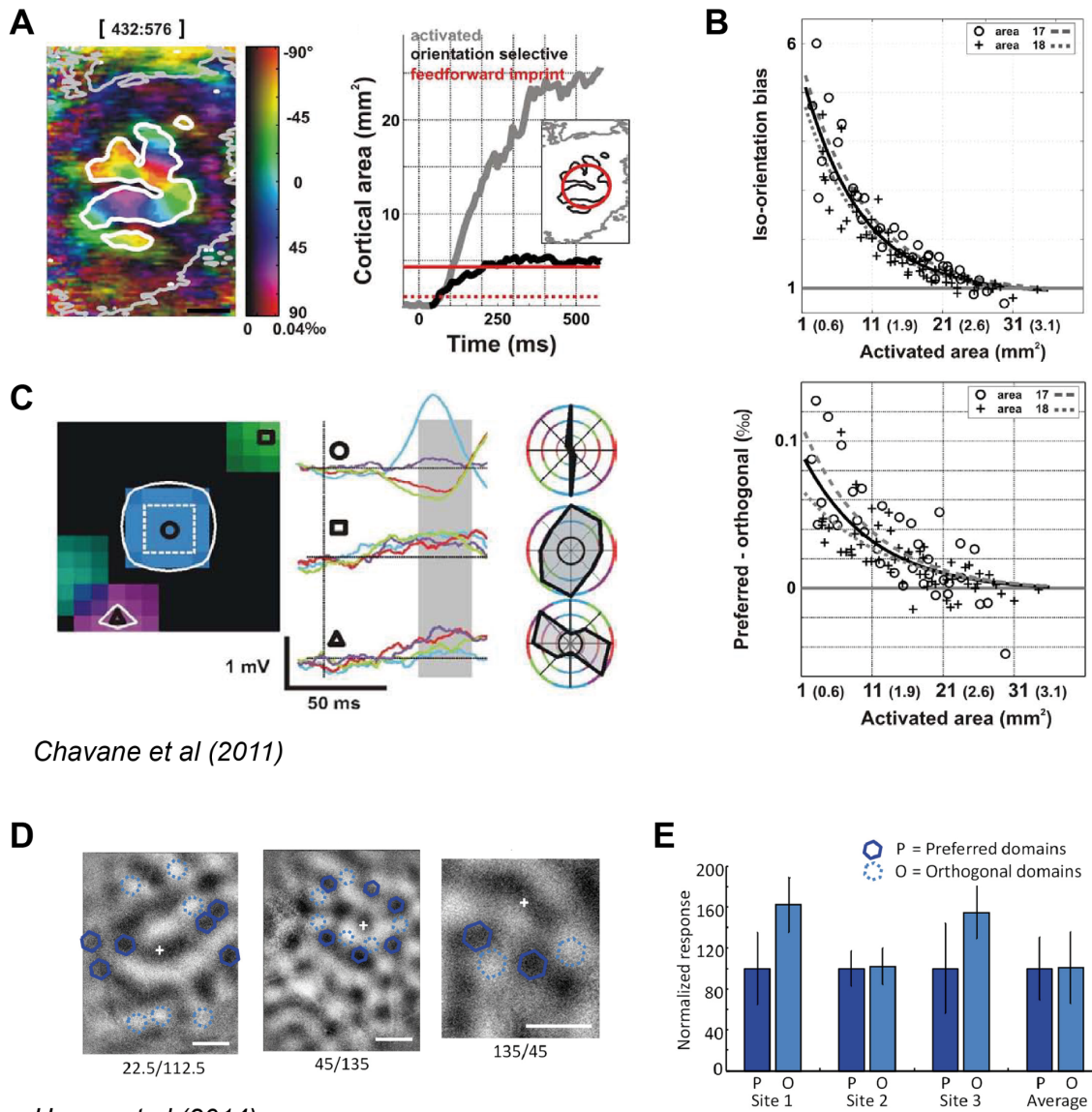
121 *Neuronal population activity measures*

122 Here, we review more recent evidence for versatile connectivity rules reported in different
123 species and with different recording techniques. Importantly, one should keep in mind that long-
124 range horizontal axons only have a subthreshold influence on their postsynaptic targets
125 (Bringuier et al. 1999). In order to study the selectivity of the postsynaptic target of these axons,
126 it is therefore important to use methods that are sensitive to subthreshold membrane potential
127 changes. Indeed, methods that only record spiking activity necessitate experimental protocols
128 that co-activate the presynaptic source and postsynaptic target of the horizontal network, to
129 study cross-correlation between neurons (Michalski et al. 1983; Ts'o et al. 1986; Schwarz and
130 Bolz 1991; Das and Gilbert 1999). Under these conditions, it is hard to tease apart the direct
131 effects of the horizontal axons rather than secondary activation of recurrent columnar circuits.

132 In 2011, Chavane and collaborators used complementary recording tools that specifically record
133 the subthreshold activity of a mesoscopic population (voltage-sensitive dye imaging, VSDI), and
134 of individual neurons (intracellular recordings) in area 17 and 18 of the anesthetized cat. The
135 first method allowed us to visualize and quantify the orientation selectivity of the laterally
136 spreading activity evoked by a local stimulus (Jancke et al. 2004). The second method enabled
137 a precise measurement of the impact of this subthreshold spread of activity on individual
138 neurons. Using VSDI in the cat area 17 and 18, the authors showed that a local oriented
139 stimulus evokes a spread of activity along the horizontal dimension, extending up to three mm
140 laterally (see also (Bringuier et al. 1999; Reynaud et al. 2012; Muller et al. 2014, 2018). It is to
141 be noted that the spread of activity did not show any patchiness, contrary to the anatomical
142 observations. However, we believe that this is to be expected considering the large variability in
143 the patches that will be activated from different neurons, varying as a function of a neuron's

144 type, layer and position in the orientation map. As a consequence, and in sharp contrast to the
145 extended horizontal activation, the orientation-selective component of this spread remains
146 confined to the cortical feedforward imprint of the stimulus (Fig. 2A). The feedforward imprint
147 being defined in Chavane et al (2011) as the population of neurons directly or partially activated
148 by the feedforward stream. This effect was systematically observed in both areas 17 and 18 and
149 quantified using complementary methods to quantify the decrease of the orientation selectivity
150 with horizontal distance. Both at the level of orientation preference and orientation selective
151 response, the bias towards like-to-like activation (and therefore functional connectivity)
152 decreases exponentially with horizontal distance with a similar characteristic cortical space
153 constant of about one mm or one hypercolumn (Fig. 2B). Importantly, this signifies, that, for a
154 lateral radius of about 1.5 mm, the iso-orientation bias (Fig2B) was in the same range as that
155 observed in the anatomy for similar lateral distance (Bosking et al. 1997, Kisvarday 1997;
156 Schmidt et al. 1997; Malach et al., 1993, Rochefort et al., 2009). However, VSDI is a population
157 measure of the subthreshold activation that pools activity from all neurons (excitatory and
158 inhibitory), all compartments (dendrite, soma and axons) and mostly the upper layer (see
159 Chemla et al 2017). Therefore, VSDI offers a unique population view of the functional activation
160 but it is less precise than anatomical studies: it is for instance possible that the lack of overall
161 bias comes from the mix of tuned and untuned subpopulations (see Kisvarday 2016 for further
162 discussion). Chavane et al (2011) therefore used intracellular recordings to confirm the VSDI
163 observations and further showed that this loss of orientation selectivity actually arises from the
164 diversity of converging synaptic inputs originating from outside the classical RF (Fig. 2C). The
165 conclusion from this work is that the lateral spread of cortical activity gradually loses its
166 orientation iso-preference at a distance of around one hypercolumn and that there exists a
167 range of strategies for different post-synaptic neurons.

168 In a more recent work, Huang et al (2014) provided similar and complementary results in a
169 different species, V1 of the tree shrew, and using a different methodological approach. The
170 authors used optical imaging of intrinsic signals to monitor the impact of intra-cortical
171 optogenetic stimulation under various stimulation configurations. In particular, their results show
172 that the optogenetic stimulation of excitatory neurons within a set of orientation domains in the
173 cortex generated the same response amplitude for either iso- or orthogonal domain stimulation
174 (Fig. 2D, E). The responses actually depended primarily on intra-cortical distance (similar to the
175 results obtained via cross-correlation in (Das and Gilbert 1999). Using their innovative
176 approach, the authors also tested stimulation along an axis in the retinotopic map, either
177 collinear with the preferred orientation or orthogonal to it. The authors found no bias in either
178 direction. Huang et al (2014) therefore provides independent and complementary evidence that
179 the horizontal network, when probed with functional measures, does not show a bias for iso-
180 orientation preference in V1. It should be noted however that using optogenetic stimulation of
181 excitatory neurons may drive complex dynamical activation of the cortex (Li et al 2019), mixing
182 excitatory and inhibitory recruitment of the lateral network with different dynamics. Since the
183 authors have used intrinsic optical imaging, they could not access to the dynamics of the lateral
184 activation that would be averaged out in the observed activation maps (see Kisvarday 2016 for
185 further discussion).

186
187

Chavane et al (2011)

Huang et al (2014)

188

189

190

191

192

193

194

195

196

197

198

199

200

Fig. 2 : Probing for the orientation selectivity of the horizontal network with functional imaging. A-C Taken from Chavane et al (2011) and D-E from Huang et al (2014). **(A)** Voltage-Sensitive Dye Imaging of the orientation selective response evoked by local oriented gratings, example from area 17 of an anesthetized cat. (Left) Polar orientation map averaged over the final 145 ms of the response (time stamps indicated above the frame). Color hue and brightness code respectively for the preferred orientation and the strength of the orientation tuning. Contours delineate the outer border of the cortical domain within which significant activation level (thin gray contour) or significant orientation selective response (thick white contour) are observed. (Right) Spatial extent of the activated area (gray) and of its orientation-selective component (black) as a function of time. Red line indicates the expected limit of the feedforward imprint, defined and estimated from Albus (1975) as the population of neurons directly or partially activated by the feedforward stream. Dotted red line indicates the retinotopic area of the stimulus representation. Inset: The spatial extent of the activation spread (gray) and the orientation-selective

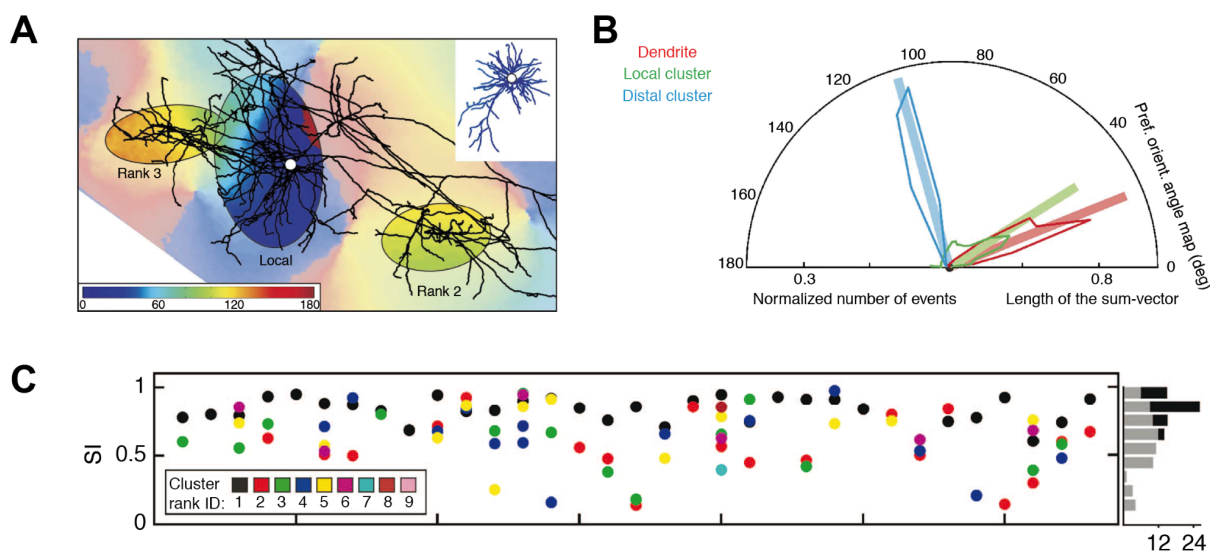
201 activation (black) are shown in comparison with the expected limit of the feedforward imprint (red). **(B)**
202 Population analysis over nine hemispheres [three in area 17 (o) and six in area 18 (+)] of the horizontal
203 distance-dependent decrease of orientation selectivity. (Top) Iso-orientation bias as a function of the
204 spatial eccentricity of the lateral spread. The first point corresponds to the area of the initial cortical
205 activation. Exponential fit is shown in black. (Bottom) Decrease in condition-wise modulation depth with
206 lateral propagation distance. **(C)** Visuotopic orientation polar map of an intracellular subthreshold
207 response; Color hue and brightness code respectively for the preferred orientation and the strength of the
208 orientation tuning. The white contours delineate the significant responsive regions when combining both
209 amplitude and orientation selectivity criteria. Middle: averaged subthreshold responses to four different
210 orientations (same color code) presented for particular locations (circle, triangle, and square); scale bars:
211 50 ms and 1 mV; Right: normalized orientation-tuning curves, integrated within a fixed temporal window
212 (shaded area of middle panel). The black circle indicates the spontaneous level for the depolarizing
213 integral measure. **(D)** Three orientation maps measured with optical imaging of intrinsic signals (Huang et
214 al 2014) with the extracellular recording site (white “+”). Optogenetic layout stimulation sites that were
215 centered over orientation domains with the same orientation preference (blue solid hexagons) as the
216 recording site (+), and stimulation sites that were centered over domains with the orthogonal preference
217 (light blue dashed hexagons). Scale bars: 500 μ m **(E)** Extracellular responses to optogenetic stimulation
218 of preferred domains (dark blue) and orthogonal domains (light blue) in the three example cases shown in
219 D, and the average responses to stimulation of preferred or orthogonal domains across all cases
220 examined (n = 10).

221 *Anatomical measures*

222 In a recent anatomical study, Martin et al (Martin et al. 2014) carefully re-evaluated the
223 orientation bias of horizontal boutons from upper layer pyramidal neurons in cat area 17 using
224 single cell intracellular labelling, optical imaging to reveal the orientation map, and advanced
225 cluster-by-cluster analysis of synaptic boutons. In their analysis, Martin et al (2014) compared
226 the distribution of the preferred orientations spanned by the neuron’s dendritic arbors (used to
227 estimate the neuron’s preferred orientation) and the preferred orientation covered by axonal
228 clusters of the neuron (Fig. 3A). In the example of Fig. 3A-B, the preferred orientation of the
229 dendrite (red) matched the one of the local cluster (green) but not of the distal cluster (blue).
230 Over 33 neurons, their results revealed a very large variability in the orientation selectivity of
231 their distal clusters (colored in Fig. 3C), as estimated by their *Similarity Index* (1 corresponding
232 to the same orientation preference distribution with respect to the neuron’s preferred orientation,
233 0 to an orthogonal orientation preference). Their results demonstrated the existence of a very
234 large variance of SI (0.13-0.96) out of all 51 clusters they observed over the 25 neurons. To test
235 whether the clusters positions within the orientation maps occur by chance, the authors made a
236 detailed bootstrap statistical analysis of all 51 clusters, taking into account the bias that is
237 introduced by the orientation map layout, the cluster size and position relative to the soma.
238 Using this analysis, they found that a quarter of their clusters (14/51 clusters recently updated to
239 17/65, personal communication from Ruesch & Martin) were not positioned randomly in the
240 map. Interestingly, only 9% (6/65) of these clusters (see their suppl Fig10I), had a significantly
241 high SI, above the upper bound (hence iso-oriented), and 5% (3/65) below the lower bound
242 (hence cross-oriented). In contrast 12% (8/65) were located in position of the orientation map
243 unlikely to occur by chance while being neither iso nor cross-oriented with the labelled cell. As a

244 conclusion, only a weak minority of clusters (9%) are significantly tuned to iso-orientation from
 245 non-random position in the orientation map. Furthermore, as shown by Buzas et al (2006), this
 246 bias tends to decrease with lateral distance of the clusters, which is further in accordance with
 247 Chavane et al (2011). Finally, as observed in Huang et al (2014), Martin et al (2014) did not find
 248 any specific alignment of the cluster distributions in the retinotopic map that could favor collinear
 249 vs orthogonal interactions with the cell's preferred orientation. At a more macroscopic level,
 250 diversity was also shown from animal to animal in tree shrew V1, specifically in the fine
 251 orientation/retinotopic arrangement of extracellular anatomical labelling (i.e. a population of
 252 neurons). In their detailed analysis (Hunt et al. 2011), showed that there is a diversity of co-
 253 circular connectivity rules across animals, some showing a significant bias towards co-circular
 254 rules, some towards anti-circular rules, and others without biases. Thus, as stated by Martin et
 255 al (2014), the horizontal axons thus cannot be treated as an homogeneous network with a net
 256 iso-oriented bias, but rather should be described as strongly heterogeneous, an heterogeneity
 257 that may be a the core of its function (see also Kisvarday 2016).

258
 259
 260



Martin et al (2014)

261
 262
 263
 264
 265
 266
 267
 268
 269
 270
 271
 272
 273

Fig. 3: Probing for the orientation selectivity of individual horizontal axons (from Martin et al 2014). **(A)** Axon of an intracellularly labelled neuron is displayed over the orientation map. Ellipses show clusters of boutons (not shown) for local and more distal positions. Dendritic tree (inset) was colour coded by the orientation value of their corresponding pixels (soma ¼ white dot). Scale bar, 0.5 mm. **(B)** Radial plots of the normalized number of boutons counted in each local (green) and distal clusters (blue) but also the dendrite (red) for each preferred orientation (coloured curves). The individual vectors forming these hemispheric plots were summed up to generate one sum-vector (bold vector). The length of this sum-vector is termed as the ‘tuning’ of the dendrite or cluster. **(C)** Similarity Index (SI) values for individual clusters of 33 neurons sorted by normalized depth of soma. (Top) neurons (xaxis) can have clusters (colour coded by rank) with different SI (yaxis). The histogram on the right summarizes the SI across clusters of all neurons (grey=distal,black=local). Note the large variance within and across neurons.

274 COMPUTATIONAL MODEL LINKING STRUCTURE TO FUNCTION

275 Population measures and anatomical data constrain connectivity in cortical space, however the
276 link between known anatomical details and the resulting functional expression (in terms of
277 neural activity) is not obvious. Computational models provide a means to explore this
278 relationship directly. Modelling studies of V1 consider a range of connectivity rules, and these
279 frequently allow for the shaping of connection strengths based on the difference of orientation
280 preference between connected sites. Abstracted models of single hypercolumns implement
281 cross-orientation interactions in local circuits that further tune selectivity derived from weakly
282 tuned LGN inputs (Ben-Yishai et al. 1995). Similar mechanisms for orientation selectivity in V1
283 have been explored in models with recurrent, lateral connections over short distances (between
284 neighbouring hypercolumns in L4) (Somers et al. 1995; Kang et al. 2003; Chariker et al. 2016).
285 Connections that extend over many mm of cortex (i.e. across multiple pinwheels) are
286 considered in visual cortex modelling studies of contextual modulation (Rubin et al. 2015),
287 motion illusions (Rangan et al. 2005), geometric visual patterns (Bressloff et al. 2001; Baker and
288 Cowan 2009; Carroll and Bressloff 2016), travelling waves (Bressloff and Carroll 2015), and in a
289 general setting (Raizada and Grossberg 2003). Whilst models do commonly feature a decay
290 (e.g. exponential or Gaussian) in the strength of orientation-based connections with distance
291 (Goldberg et al. 2004; Blumenfeld et al. 2006), the tuning strength is not distance dependent,
292 rarely systematically investigated and not constrained by anatomical data. The function of
293 patchy long-range connections has further been investigated in contexts not specific to
294 orientation encoding (Voges et al. 2010; Voges and Perrinet 2012). In general, long-range
295 connections feature a strong iso-orientation bias motivated by long-held assumptions that do not
296 take into account the more recent functional and anatomical studies that motivate a modification
297 of this rule.

298 A common modelling choice for local excitation-inhibition connectivity is a so-called Mexican-hat
299 with inhibition extending further than excitation (Marr and Hildreth 1980; Grossberg 1983;
300 Somers et al. 1995; Bressloff et al. 2001). This choice is known to generate stable localised
301 patterns of activity (rather than spatial unstable dynamics that spreads across cortex) (Laing
302 and Troy 2003), however, excitatory connections in V1 can extend many mm further than the
303 local inhibitory footprint. In general, models that also feature long-range excitation are used to
304 study unbounded patterns of activity rather than localised responses to inputs (Bressloff et al.
305 2001; Blumenfeld et al. 2006). (Rankin et al. 2014) extended the results of (Laing and Troy
306 2003) to demonstrate that localised inputs can generate stable localised activity patterns (rather
307 than spreading activity) with a connectivity rule (as suggested in (Buzás et al. 2001), and similar
308 to Fig. 4A) that features long-range excitation, extending much further than the local inhibitory
309 network.

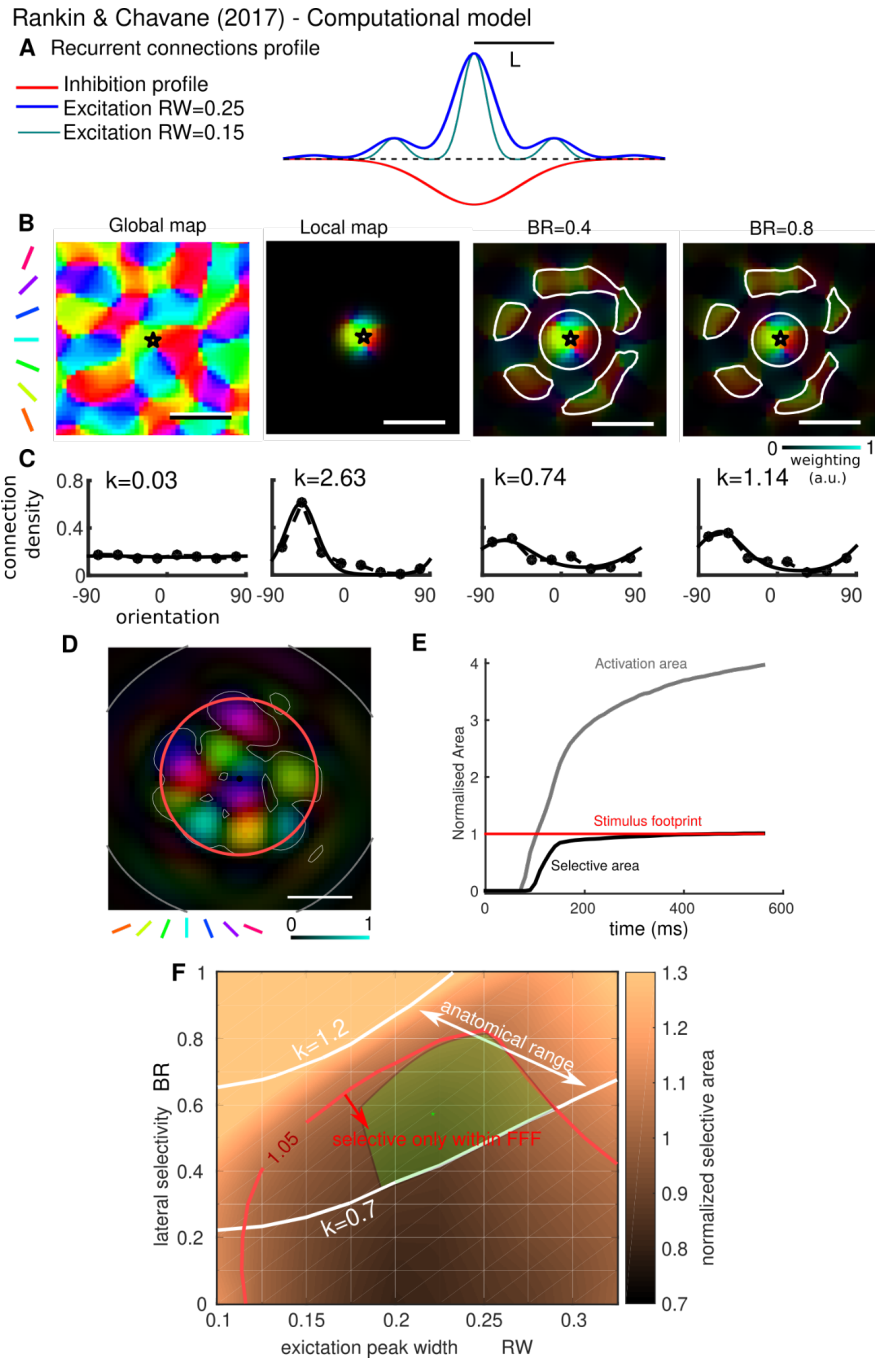
310 (Rankin and Chavane 2017) developed a planar spatial model of orientation-selective activation
311 in V1 L2/3 with the aim of bridging between known anatomical constraints on the tuning of long-
312 range connections (Buzás et al. 2006) and the functional expression of laterally propagating
313 activity driven by localised stimuli (Chavane et al. 2011). A neural field architecture with
314 orientation-specific sub-populations provides a mesoscopic description of neural activity, ideal

315 for comparison with the temporal and spatial resolution in VSDI imaging experiments. A novel
316 connectivity function was flexibly parametrized to investigate clustering of connections, their
317 orientation bias and balance between excitation and inhibition. We adopted the non-orientation
318 specific nature of local excitatory connections (Buzás et al. 2006) and inhibitory connections
319 (Buzás et al. 2001); see also (Koch et al. 2016) for a discussion of orientation specificity of
320 excitatory and inhibitory connections. Taking motivation from (Buzás et al. 2001), longer-range
321 excitatory connections are proposed here to, although decaying with distance, form in rings at
322 multiples of the hypercolumn separation L (Fig. 4A). This allows for the following important
323 features to be captured: that excitatory connections 1) drop in number at a range of $L/2$, 2) have
324 a peak at a range of L (and multiplies therefore) and 3) can extend several mm across cortex.
325 Two parameters were tuned to agree with the available data from (Buzás et al. 2006), the width
326 of peaks in number of excitatory connections (RW ; two values shown in Fig. 4A) and their
327 orientation bias (BR ; illustrated in Fig. 4B-C).

328 We found a significant overlap between the anatomically relevant parameter range and patterns
329 of cortical activation consistent with imaging experiments (Chavane et al. 2011). Hence, this
330 computational approach allowed us to reconcile the imaging results with the reported level of
331 orientation bias from anatomical studies. Specifically, (Chavane et al. 2011) found a sharp
332 decay of orientation selective activation at the stimulus retinotopic footprint border, resulting in
333 peripheral activation that was not orientation selective. Our results demonstrate that this sharp
334 decay is contingent on three factors: the diffuse clustering of long-range connections, the
335 intermediate range (consistent with anatomy) of their orientation bias and sufficient balance
336 between excitation and inhibition. It is worth noting that orientation-biased long-range
337 connections can recruit a local non-orientation-biased network at the target, resulting in non-
338 orientation specific activation (Huang et al. 2014). The modelling work illustrates that the
339 observed levels of orientation bias in anatomical studies actually predict long-range activation
340 beyond the retinotopic stimulus footprint with a sharply decaying orientation selectivity profile.

341 The model offers further insights into the mechanistic value of excitatory-inhibitory balance, and
342 of intermediate levels of orientation bias in long-range connections. Long-range excitatory
343 connections (reaching much further than the lateral inhibitory profile) could easily lead to
344 destabilization of activity generated by localised visual stimuli. Our model was used to show that
345 if the orientation bias of lateral connections is excessively strong, or if inhibition is particularly
346 weak, the network operates close to an instability leading to unbounded cortical activation. This
347 provides another line of evidence in favour of distance-decaying orientation bias in lateral
348 connections. Diversity of long-range connections increasing with distance (i.e. decreasing
349 orientation bias with distance) reflects a potential need to activate a broader range of
350 orientations as we move further from a local stimulus with a specific orientation. Furthermore,
351 the fact that, under particular circumstances, the preferred orientation of the horizontal
352 propagation may be at odds with the underlying orientation preference map could unravel some
353 new unexpected computational capacities of the horizontal network, which may be present in
354 visual areas beyond V1. For instance, the ability to link information across position and
355 orientation for non co-circular filters, which is important for processing objects with sharp angles.
356 In line with this hypothesis, (Chavane et al. 2011) showed that the spread of orientation

357 selective activity is not fixed but can increase with increasing spatial summation generated by
 358 annular stimuli.
 359



360
 361

362 **Fig. 4: Neural field model to reconcile structure with function in primary visual cortex.** Definition of
 363 model connectivity with anatomical constraints (**A-C**) and illustration of model behaviour with operating
 364 region in agreement with functional characteristics (**D-F**). (**A**) Radial connectivity profile for inhibition
 365 (Gaussian decay) and excitation (locally Gaussian decay, longer range connections peak in number at
 366 distance L and multiples thereof). Ring width (RW) of peaks in excitatory connections illustrated for two

367 values. **(B)** Example of local preference map and resulting lateral connectivity for two values of the
368 orientation bias of recurrent connections (BR). **(C)** Orientation tuning for each panel in **B** above (circles)
369 with tuning parameter k from a best-fit von-Mises distribution (solid lines). Orientations are evenly
370 represented in the global map but strongly biased at around -60° for the local excitatory component (*local*
371 *map*). The orientation bias of lateral connections increases to around $k=1$ for $BR>0.5$ (similar values
372 reported in (Buzás et al. 2006)). **(D)** Model simulation snapshot at 600ms showing the orientation-
373 selective component within a thin white contour, confined to the feedforward footprint FFF of the stimulus
374 in red; the much broader non-orientation-specific activity falls within a grey contour extending beyond the
375 plot limits. **(E)** Time history of the area within the non-orientation-specific contour and the orientation-
376 selective contour. **(F)** Colour map across range of RW and BR values showing the selective area as in **D**
377 normalised by FFF. Within the red contour the selective activation is constrained to the FFF. White
378 contours show the anatomically constrained range for the connectivity parameters RW and BR where
379 $k=0.7-1.2$. In the green region other constraints on the correct orientation and the radial decay rate of
380 orientation selectivity are also satisfied (details in (Rankin and Chavane 2017)).
381

382 FUNCTIONAL ADVANTAGES OF SUCH AN ORGANIZATION

383 The insights we have reviewed at the physiological and modeling levels support a range of
384 novel hypotheses for the organization of long-range lateral connectivity in the primary visual
385 cortex. A functional approach, asking "*why should neurons in V1 be connected laterally?*"
386 provides a complementary perspective. Indeed, a major argument is that the structure of V1
387 should fulfill its function and implement principles of perceptual organization, such as the
388 principle of *good continuation* to bring a contour's constituent edges together into a unified
389 global percept (Wertheimer 1923). How might these principles connect knowledge across
390 anatomy, physiology, theory, and modeling?
391

392 *Principles of perceptual organization in natural images*

393
394 A major constraint for neurons in the primary visual cortex is that information is encoded locally
395 in their activity and must be integrated globally across the visual field. Surprisingly, perceptual
396 principles organizing the different fragments of an image can be directly extracted by analyzing
397 a database of natural images. One such principle is that pairs of edges in natural images are
398 most likely organized along aligned contours, and more generally on a common circle (Sigman
399 et al. 2001); the authors extracted edges from natural images and estimated the orientation of
400 each edge. For each pair of active edges, they showed that the angle of maximum interaction
401 corresponds to a configuration for which they are close to co-circular. This long-range
402 correlation is a marker of the structure of natural images and may provide strong prior
403 knowledge for the perceptual organization of low-level features.
404

405 Such a structural prior can be described as a form of "association field" extending the concept of
406 a neural receptive field to long-range local interactions. The seminal paper by Field (Field et al.
407 1993) defines the association field as the set of local oriented elements (edges) in the visual

408 field that facilitates the detection of a central oriented target. They showed that the association
409 field obeyed a co-circular rule. In other words, if a common circle can pass through the central
410 target and the peripheral element, they will facilitate each other's detection, and generate
411 suppression otherwise. This association field is invariant to translations or rotations. It extends
412 the prior of collinearity (like-to-like) or co-circularity (Sigman et al. 2001) to a more generic
413 description of all possible co-occurrences. In particular, by exploring the interactions of edge
414 pairs, they showed that these association fields explain the detection of paths embedded within
415 a field of randomly oriented edges. The association field can then be understood in light of the
416 computer vision problem of curve tracing. Parent and Zucker (1989) described it as a diffusion
417 process over the tangent field of oriented edges, thus suggesting a principled and biologically
418 realistic framework for association fields using long-range interactions.

419

420 This principle can be extended to explain psychophysical experiments in humans. Geisler et al.
421 (2001) took a similar approach by reporting the full statistics of natural image edge co-
422 occurrences. This yields a valuable model for the statistics of neighboring edges. First, the
423 edges are organized into parallel textures favoring parallel edges, and second, there is a bias
424 for co-circular edges (see Fig. 5A). Using a Bayesian approach, the authors derived a clustering
425 scheme for chaining edges into contours that was confirmed by psychophysical experiments.
426 This approach was later extended to the high-level cognitive problem of image categorization
427 (Perrinet and Bednar 2015). The authors showed that using supervised learning, one could
428 derive a scheme using the association field in that image to categorize whether it contains an
429 animal. This simple model achieved similar performance to humans and to a deep hierarchical
430 model (Serre et al. 2007). Surprisingly, the model made similar errors to humans. This illustrates
431 first that association fields can be used to both group edges based on different tasks or to
432 categorize images. This also shows that for the association field reflecting the statistics of edge
433 co-occurrences in natural images, different datasets may lead to different association field
434 structures (see Fig. 5A). As a consequence, it seems relevant at behavioral and ethological
435 levels that mechanisms exist to tease apart the slight differences between the co-occurrence
436 patterns present in different images, for instance the surprising patterns of a perfect co-
437 circularity, or that of a pair of rare but informative orthogonal edges forming a T-junction. This
438 would then explain part of the variability in the association fields which can be involved in visual
439 integration processes.

440

441 *How do these principles translate to the cortical space?*

442

443 As Geisler (2001) states, "*the obvious hypothesis for the local grouping is a neural population*
444 *with the receptive field structure matched to the edge co-occurrence statistics*". Yet, the
445 emergence of receptive field properties is a combination of anatomy and the dynamics of
446 individual neurons. Can we link the statistics of natural images to the structure of processing in
447 the primary visual cortex?

448

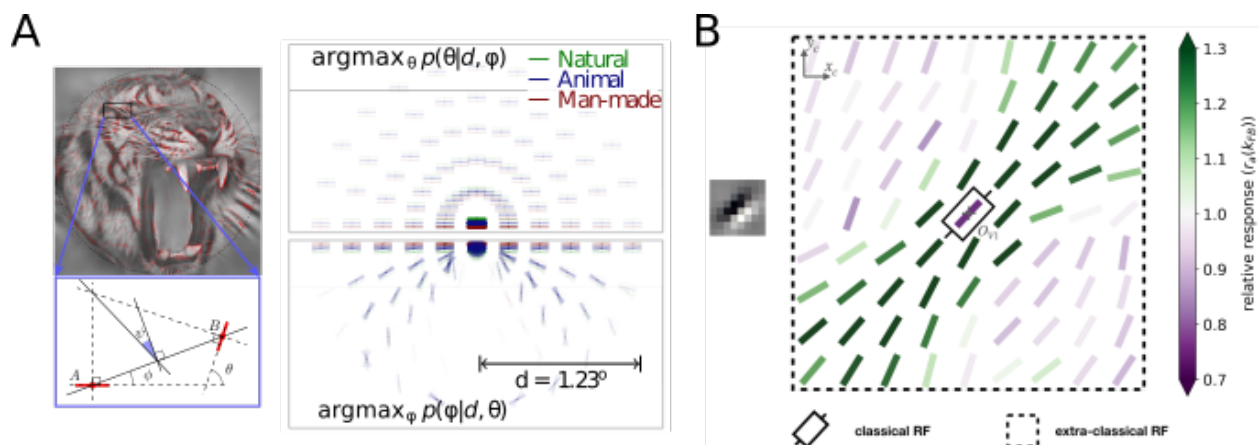
449 Olshausen and Field (1996) set out to show how the structure of V1 microcolumns can optimize

450 the efficiency of the neural representation for natural images. Hyvärinen and Hoyer (2001)
 451 extended this to include a regularization of the representation with cortical topography.
 452 Franciosi et al (2021) recently developed a biologically realistic, two-layered V1 sparse
 453 predictive coding model including pooling mechanisms to impose a neighborhood prior in
 454 cortical space, which includes by construction the possibility of representing as channels in each
 455 layer a variety of interaction patterns. Similarly, complex cells and topographic maps emerge,
 456 demonstrating the transfer of cortical connectivity in V1 to perceptual grouping principles. More
 457 surprisingly, depending on the density of neurons, different structures emerge to optimize cost
 458 efficiency: in addition to mammalian-specific features (such as topographical maps), a rodent-
 459 specific salt-and-pepper map emerges for models with a lower cell density. Interestingly, by
 460 focusing on this multi-channel convolutional architecture, the second layer showed a diversity of
 461 connectivities across channels, suggesting that differing anatomical constraints may induce
 462 different patterns of long-range lateral interactions.

463

464 A multi-layer sparse predictive coding model (Boutin et al 2020) allows for the influence of an
 465 extrastriate cortical area such as V2 on to V1 to be modelled. The activity in the layers of this
 466 model emerge from the recurrent interactions between neurons within and across layers (rather
 467 than a feed-forward pass as in convolutional networks). Convergence to an efficient
 468 representation of edge filters and interaction maps (resembling association fields) emerges after
 469 several processing iterations. However, training on different natural image datasets can produce
 470 different interaction maps, in accordance with Perrinet and Bednar (2015). For example, training
 471 on images of human faces generated features resembling mouths or eyes, resulting in more
 472 sparse and longer range interactions. This suggests that instead of a simple similarity rule,
 473 lateral interactions between neurons reflect the variety of feature dependencies attached to the
 474 respective neurons. In addition, similarly to physiological observations (Gilbert and Li, 2013) we
 475 observed that the interaction becomes sharper with stronger feedback (see Fig. 5B), which
 476 proves a synergy between the different pieces of information encoded by the network, as
 477 illustrated by improved performance for denoising natural images.

478



479

480 Fig. 5: Function and diversity of Association Fields. (A) Following the work of (Geisler et al. 2001), one
 481 could derive the association field from the statistics of natural images. This involves extracting edges from
 482 images (red segments) and computing for each pair the difference of angle θ and the relative azimuth ϕ of

483 *one edge compared to the other. This allows to quantify the association field as the histogram, relative to*
484 *a reference edge placed in the middle, for the most likely difference of angle - showing a prominent*
485 *preference for parallel textures (top) or the relative azimuth, showing a prior for co-circular co-occurrences*
486 *(bottom). The association field may vary for different databases with an excess of co-circularity in images*
487 *containing animals, illustrating the variety of statistics faced by the visual system (Perrinet and Bednar*
488 *2015; modified with permission CC-BY). (B) Boutin et al (2020) describes a biologically realistic multi-*
489 *layer model of the visual cortex. The model is shown natural images and is optimized to represent images*
490 *in the most efficient way. Edge-like filters emerge (see an example in the inset) and we show here the*
491 *interaction of this edge with other edges outside the range of its classical receptive field. This pattern*
492 *shows a large facilitatory (green) or inhibitory (purple) effect relative to a model without feed-back. This*
493 *functional modulation of the association field shows the importance of the activity in the whole network*
494 *and we have further shown its shape could widely vary within the network and for different types of*
495 *images, such as images of faces (Boutin et al 2020; modified with permission CC-BY).*

496 *Function and dynamics of long-range lateral interactions*

497 Overall, these theoretical models propose, as an alternative to the like-to-like structure, that
498 there should be a wide variety of long-range lateral interaction patterns. It should be noted that
499 most of the models described above deal with static natural images, whereas the visual world is
500 characterized by a wealth of different dynamic scales, which raises the question of the role of
501 neural dynamics in long-range lateral interactions.

502

503 If one imagines an edge moving in a direction parallel to its orientation, we can infer that we are
504 following the tangent to a continuous contour. On the contrary, if the orientation of the edge is
505 perpendicular to its direction, it is more likely that we are seeing a moving bar. This simple
506 prototypical example shows that depending on the local intrinsic context, the optimal integration
507 rule may change, as evidenced by intracellular recordings (Gerard-Mercier et al. 2016). If these
508 interactions can be implemented via different contextual cues such as recurrent or feedback
509 connections, it is also possible that the multidimensional representation of information on the
510 cortical surface is much more than a simple topographical orientation map.

511

512 In addition, there is physiological evidence that association maps can be dynamically influenced
513 by the task at hand. In (McManus et al. 2011), using a delayed-to-sample matching task, the
514 authors trained monkeys to detect different patterns: a circle, a wiggle, or a line, which were
515 embedded in a grid display of randomly oriented edges similar to that of (Field et al. 1993). They
516 found that depending on the pattern being searched, the recorded association field adapted to
517 preferentially exploit collinearities (for lines) or co-circularities (for circles). Such a differential
518 processing raises an implementation problem for the unsupervised schemes described above.
519 This problem could be solved in a supervised learning scheme (Perrinet and Bednar 2015) but
520 raises the question of how this supervised credit is assigned in V1. A similar problem is inherent
521 in the backpropagation rule in generic deep learning paradigms which can be solved in a
522 predictive coding framework (Boutin et al. 2021).

523

524 Lastly, the anatomical connectivity may be patchy for different functions than just connecting
525 like-to-like orientation patches. Indeed, patchy connections likely play an important role in

526 combining information from multiple visual cues beyond orientation, including context (Martin et
527 al 2017). Indeed, modelling work has shown that patch-based connectivity increases the
528 versatility of the dynamic repertoire of neural states (Voges et al, 2010). That work compared
529 networks of realistic conductance-based neurons with a range of connectivity rules. These rules
530 had different complexities, from a completely random connectivity, to a neighborhood-based
531 local connectivity, and more interestingly, clustered networks including a patch-based
532 connectivity rule. This was extended in a further modelling work (Voges and Perrinet, 2012) to
533 include a comparison between a pure random patch-based connectivity and partially
534 overlapping patches. As noted in (Kisvárdy 2016), these patch-based connectivity rules were
535 sufficient to induce a large dynamic repertoire such as rhythms or travelling waves and was for
536 instance characterized by enhanced variety in the shape of the power spectrum of population
537 activity. In particular, such a range of dynamic behaviours is much richer when compared to
538 those obtained with a random or local connectivity rule. Patchy connectivity rules introduce a
539 heterogeneity in the lateral connections, which seems essential for building up an efficient
540 population code (Martin et al 2014). In particular, this would allow the propagation of
541 combinations of contextual cues which would reflect the richness of visual information in natural
542 scenes.

543

544 To conclude this section, the function studied in these theoretical models hints at a solution
545 using a superposition of different long-range connectivity profiles. The diversity of patterns and
546 their adaptability to the task or statistics should overall improve processing efficiency in the
547 primary visual cortex. Yet there remain open questions regarding the richness of these like-to-all
548 patterns. Theories suggest potential strategies for addressing these open questions explicitly in
549 neurophysiology, for example by synthesizing optimally responsive, model-driven dynamic
550 stimuli (Walker et al. 2019).

551 DISCUSSION

552 In this review, we have documented convergent evidence from physiology, anatomy and
553 computational models that the orientation selectivity of horizontal network connectivity in the
554 primary visual cortex of carnivores, ungulates and primates is more versatile than initially
555 proposed, leading to the necessity to revisit the like-to-like connectivity rule (Mitchison & Crick
556 1982) still dominant today. At the anatomical level, there seems to be a diversity of connection
557 rules between presynaptic source and postsynaptic target. At the individual cell level,
558 anatomical studies have shown that the rule changes as a function of cell type (excitatory vs
559 inhibitory) and layer/map locations (Yousef et al. 2001, Kisvárdy et al. 1994; Buzás et al. 2001,
560 Yousef et al. 1999; Karube and Kisvarday 2010; Karube et al. 2017). Within one presynaptic
561 origin, a large diversity exists with only moderate bias in the range of 1.5-2 times greater than
562 chance (Bosking et al. 1997, Kisvarday 1997; Schmidt et al. 1997; Malach et al., 1993,
563 Rochefort et al., 2009), More recent work by Martin et al (2014) on the upper layer pyramidal
564 neurons of the cat V1 with a cluster-by-cluster analysis of horizontal boutons has shown the
565 existence of a very large diversity from like-to-like, like-to-any, like-to-all and like-to-unlike
566 connectivity rules. Altogether no net significative bias towards one of these rules could be
567 observed in their bootstrap statistical analysis. Taken together, these anatomical results show

568 that there is diversity in the connectivity rules both within and between neuronal types and
569 locations (see Kisvarday 2016 for an extensive review). At a more macroscopic level, it is
570 interesting to note that Hunt et al (2011) also observed that the co-circularity rule is different
571 from animal to animal.

572

573 When probed with functional measures of neuronal activity, in response to a local visual
574 stimulus using techniques sensitive to subthreshold membrane potential fluctuations (Chavane
575 et al 2011) or an optogenetic activation of specific orientation columns (Huang et al 2014), the
576 diversity revealed in anatomical studies leads to the absence of net bias towards like-to-like
577 interactions along the horizontal network (see Alonso & Kremkow 2014), but also the absence
578 of patchy activation of the horizontal spread of activation. Importantly, VSDI measures
579 demonstrate a clear exponential decay of the like-to-like connectivity bias with horizontal
580 distance, an effect also observed in anatomy (Buzas et al 2006, Martin et al 2014). At short-
581 range distances, similar iso-orientation biases, as reported in anatomical studies, were
582 observed. However, after the equivalent of one hypercolumn, no significant bias could be
583 observed (Chavane et al 2011).

584

585 All these papers therefore demonstrate the existence of a connectivity rule that links neurons in
586 the primary visual cortex depending on their preferred orientation, neuronal type and position
587 (layer and orientation map) and intra-cortical distance. This multidimensional connectivity rule is
588 also subject to large diversity not just from neuron to neuron but also from animal to animal. Due
589 to the difficulty in making predictions from this complex pattern, it is necessary to use
590 computational approaches to probe for the expected functional behavior of such a network. In
591 Rankin & Chavane (2017), we developed a neural-field model and demonstrated that the
592 functional results observed in Chavane et al (2011) are indeed the expected mesoscopic
593 behavior of such a network when its connectivity is constrained to match the orientation bias of
594 connections from anatomy (Buzás et al. 2006), thus demonstrating that the functional
595 observations are to be expected given our understanding of anatomical characteristics.

596

597 In this review, we wish to update the accepted like-to-like connectivity rule widely assumed as
598 the building block for connecting a local neuronal network from one position in the visual field to
599 its postsynaptic targets. The connectivity rule should be revised to a distance-dependent
600 formulation: **from like-to-like bias at short horizontal distance to like-to-all at long**
601 **horizontal distance (Fig. 1E)**. The space constant of the decrease of the like-to-like bias is
602 about one hypercolumn distance. Functionally we can speculate that this translates to an iso-
603 orientation bias for neurons with overlapping receptive fields and no net bias for neurons with
604 non-overlapping receptive fields.

605

606 This may be at odds with the well-documented association field schema and co-circularity rules
607 observed in natural scenes (Sigman et al. 2001, Geisler et al. 2001). However, it is important to
608 differentiate the basic connectivity building block, that specifies unidirectional rules from a
609 presynaptic region to a postsynaptic target, from lateral interactions, that are evoked by more
610 complex stimuli that co-activate both presynaptic and postsynaptic regions (e.g., as in cross-
611 correlation studies). The like-to-all long-distance connectivity rule can be seen as generic and

612 allows for a variety of interactions in the orientation and spatial domain. Importantly, this is
613 possible if we take into account the large local diversity observed at neuronal level (Chavane et
614 al 2011, Martin et al 2014, see also Monier et al 2003). Our proposition here is that such a rule
615 could account for a wealth of interaction rules depending on the stimulus and/or the task. For
616 instance, this would allow to account for the interactions necessary to process orientation
617 discontinuities such as junctions or corners. Neurons in V1 have indeed been reported to be
618 sensitive to orientation discontinuities, independent to the absolute orientation of the stimulus -
619 set (Sillito et al. 1995, Jones et al 2001). This result could not be explained solely by iso-
620 oriented lateral interactions. Such diversities could also contribute in shaping the orientation
621 tuning of neurons away from primary orientation preference (i.e. horizontal and vertical
622 orientations, Vidyasagar & Eysel 2015). More generally, using natural, stationary scenes and/or
623 contour integration tasks may indeed favor association field interactions. However, depending
624 on the type of natural images, Perrinet & Bednar (2015) have shown that these interactions may
625 already differ significantly (see also Boutin et al. 2021). Moreover, dynamic non-stationary visual
626 stimuli, such as a simple moving object, and tasks that rely on motion integration for instance,
627 could lead to different associative rules for motion (Gerard-Mercier et al. 2016). In the case of
628 integrating information along a coherent path for instance, visual information should be
629 transported in the direction of motion (Perrinet and Masson, 2012) that can be in the cross-
630 orientation dimension.

631

632 Importantly, co-circularity rules that link orientation and position with respect to a central
633 oriented feature, are not found in the anatomy (Martin et al 2014, Hunt et al 2011), nor where
634 they found by Huang et al (2014) using optogenetic stimulation of pattern in the horizontal
635 network. This further supports a dynamic, context-dependent emergence of specific rules, such
636 as co-circularity for contour integration in natural images, through higher-order network
637 interactions. In that respect, Chavane et al (2011) observed that increasing the spatial
638 summation of the stimulus increases the propagation of iso-orientation activity, even if the basic
639 connectivity profile was shown to be not selective to orientation at long-range. This means that
640 from a basic unselective building block, selective interaction can occur (for a proposition of
641 possible mechanisms see Chavane et al (2011)). This effect could result from the fact that
642 inhibitory neurons tend to make more horizontal connections with neurons with different
643 orientation preference than excitatory neurons (Kisvárdy et al. 1994; Buzás et al. 2001).
644 Increasing spatial summation could change the orientation-dependence of the
645 excitatory/inhibitory balance and lead to the emergence of tuned activity at longer distance.
646 More generally, the emergence of new selectivity depending on the stimulation pattern (or the
647 task) is rendered possible by the existence of local diversity of orientation selective connections
648 at neuronal level (Monier et al. 2003; Chavane et al. 2011; Martin et al. 2014). Therefore,
649 different stimulation patterns will lead to activation of different recurrent subnetworks and the
650 emergence of a variety of selectivity characteristics. It is indeed now well documented that non-
651 trivial, paradoxical effects, can arise from recurrent balanced networks (Tsodyks et al. 1997;
652 Ozeki et al. 2009; Pattadkal et al. 2018). In our model, we indeed observed that manipulating
653 the balance between excitation and inhibition (i.e. reducing inhibition strength), predicts the
654 emergence of spurious orientation selective activation through long-range lateral connections
655 (Rankin & Chavane 2017).

656

657 Given the non-trivial effects that can arise with more complex stimuli, a number of avenues
658 remain open to build on theoretical and modelling work. The model developed in (Rankin and
659 Chavane 2017) could also be used to investigate selective recruitment and spatial summation in
660 regions between localized oriented stimuli (Chavane et al. 2011; Huang et al. 2014). Indeed,
661 increasing spatial summation increases the slope of selectivity decay at the stimulus boundary,
662 whilst selective propagation reaches further across cortex, a property easily explored in the
663 model by a more diverse class of localised stimuli. More generally, the model could be used to
664 make predictions to decipher the selective functional connectivity rules that link position and
665 orientation in cortical space. Importantly, it could also be extended to differentiate inhibitory cell
666 subclasses as reported in (Buzás et al. 2001). As such it could generate functional predictions
667 on e.g. the role of long-range basket cell connections that preferentially target cross
668 orientations. Extending the framework further, a feature space including spatial frequency (SF)
669 could be used to investigate lateral connections in light of recent work on interactions between
670 orientation and spatial frequency maps (Romagnoni et al. 2015; Ribot et al. 2016).

671

672 In this review, we mostly focus on revisiting the connectivity rule of intra-cortical horizontal
673 networks. However, it is important to consider that such connectivity patterns can also be
674 influenced by feedback from higher cortical areas that provides a more diffuse and divergent
675 input to the primary visual cortex (Salin et al., 1989, 1992). Anatomical studies in the cat,
676 suggest that area 17 and area 18 cells are preferentially connected when they share similar
677 preferred orientations (Gilbert and Wiesel, 1989). In the monkey, feedback from higher areas
678 (V2 and V3) to V1 show variable level of patchiness (Stettler et al 2001; Angelucci et al 2002),
679 unselective to orientation (Stettler et al 2001). In the cat, electrophysiological and inactivation
680 studies of various downstream areas seems rather to influence only response amplitude or
681 tuning width of neurons in area 17 of the cat (Martinez-Conde et al., 1999, Wang et al., 2000,
682 2007; Huang et al., 2004; Liang et al., 2007; Shen et al., 2008, Huang et al., 2007, Galuske
683 et al., 2002; Shen et al., 2006). However, it is important to consider that feedback will interact
684 with horizontal network as demonstrated in monkey visual cortex, with either specific
685 interactions as suggested by CD Gilbert (Gilbert & Li 2013 for review), or contributing to center-
686 surround processing (Hupé et al 1998, Roberts et al (2007) Poort et al 2012, Nurminen et al
687 2018).

688

689 In conclusion, we believe that there are enough arguments today to accept a change of
690 connectivity rules for horizontal axons in V1, that is consistent with both new structural and new
691 functional evidence. It remains to be established how this complex multidimensional rule
692 (orientation x distance x neuron type x neuron location) is put into play out under different
693 stimulus and task configurations. It would be important to understand what is the minimal
694 stimulus design that can trigger particular tuned interactions for various spatial positions and
695 whether it involves precisely the same neurons in the network. To test predictions that can arise
696 from theoretical and computational approaches, new experimental tools to visualize large
697 massive neural networks at neuronal level and sensitive to membrane potential fluctuations will
698 be needed. Recent neuro-technological advances in awake animals, such as all-optical tools to
699 measure and control a large set of neurons (Ju et al. 2018, Zhang et al. 2018), and the

700 development of new genetically-encoded voltage indicators that allow simultaneous two-photon
701 microscopy subthreshold activity recording from many cells (Villette et al. 2019), provide the
702 ideal experimental setting to probe the complex and dynamic network interactions underlying
703 stimulus and task-dependent processing.
704

705 **Declarations**

706 Funding (information that explains whether and by whom the research was supported) : LP and
707 FC are supported by CNRS and AMU and ANR “HorizontalV1” ANR-17-CE37-0006-02.

708 Conflicts of interest/Competing interests (include appropriate disclosures): The authors have no
709 relevant financial or non-financial interests to disclose.

710 Availability of data and material (data transparency): Not applicable

711 Code availability (software application or custom code): Not applicable

712 Authors' contributions: All authors contributed equally to the review.

713 Additional declarations for articles in life science journals that report the results of studies
714 involving humans and/or animals: Not applicable beca
715

716 **References:**

717 Alonso J-M, Kremkow J (2014a) Faculty Opinions recommendation of Optogenetic assessment
718 of horizontal interactions in primary visual cortex. Faculty Opinions – Post-Publication Peer
719 Review of the Biomedical Literature

720 Alonso J-M, Kremkow J (2014b) Faculty Opinions recommendation of Lateral Spread of
721 Orientation Selectivity in V1 is Controlled by Intracortical Cooperativity. Faculty Opinions –
722 Post-Publication Peer Review of the Biomedical Literature

723 Baker TI, Cowan JD (2009) Spontaneous pattern formation and pinning in the primary visual
724 cortex. *J Physiol* 103:52–68

725 Ben-Yishai R, Bar-Or RL, Sompolinsky H (1995) Theory of orientation tuning in visual cortex.
726 *Proceedings of the National Academy of Sciences* 92:3844

727 Blumenfeld B, Bibitchkov D, Tsodyks M (2006) Neural network model of the primary visual
728 cortex: from functional architecture to lateral connectivity and back. *J Comput Neurosci*
729 20:219–241

730 Bosking WH, Zhang Y, Schofield B, Fitzpatrick D (1997) Orientation selectivity and the
731 arrangement of horizontal connections in tree shrew striate cortex. *J Neurosci* 17:2112–
732 2127

733 Boutin V, Franciosini A, Chavane F, et al (2021) Sparse deep predictive coding captures
734 contour integration capabilities of the early visual system. *PLoS Comput Biol* 17:e1008629

735 Braitenberg V (1962) A note on myeloarchitectonics. *J Comp Neurol* 118:141–156

736 Bressloff PC, Carroll SR (2015) Laminar Neural Field Model of Laterally Propagating Waves of
737 Orientation Selectivity. *PLoS Comput Biol* 11:e1004545

- 738 Bressloff PC, Cowan JD, Golubitsky M, et al (2001) Geometric visual hallucinations, Euclidean
739 symmetry and the functional architecture of striate cortex. *Philos Trans R Soc Lond B Biol*
740 *Sci* 356:299–330
- 741 Bringuier V, Chavane F, Glaeser L, Frégnac Y (1999) Horizontal propagation of visual activity in
742 the synaptic integration field of area 17 neurons. *Science* 283:695–699
- 743 Buzás P, Eysel UT, Adorján P, Kisvárdy ZF (2001) Axonal topography of cortical basket cells
744 in relation to orientation, direction, and ocular dominance maps. *J Comp Neurol* 437:259–
745 285
- 746 Buzás P, Kovács K, Ferecskó AS, et al (2006) Model-based analysis of excitatory lateral
747 connections in the visual cortex. *J Comp Neurol* 499:861–881
- 748 Carroll SR, Bressloff PC (2016) Phase equation for patterns of orientation selectivity in a neural
749 field model of visual cortex. *SIAM J Appl Dyn Syst* 15:60–83
- 750 Chariker L, Shapley R, Young L-S (2016) Orientation Selectivity from Very Sparse LGN Inputs
751 in a Comprehensive Model of Macaque V1 Cortex. *Journal of Neuroscience* 36:12368–
752 12384
- 753 Chavane F, Sharon D, Jancke D, et al (2011) Lateral Spread of Orientation Selectivity in V1 is
754 Controlled by Intracortical Cooperativity. *Front Syst Neurosci* 5:4
- 755 Chemla S, Muller L, Reynaud A, Takerkart S, Destexhe A, Chavane F. 2017. Improving voltage-
756 sensitive dye imaging: with a little help from computational approaches. *Neurophotonics*
757 4:031215. doi:10.1117/1.nph.4.3.031215
- 758 Creutzfeldt OD, Garey LJ, Kuroda R, Wolff JR (1977) The distribution of degenerating axons
759 after small lesions in the intact and isolated visual cortex of the cat. *Exp Brain Res* 27:419–
760 440
- 761 Das A, Gilbert CD (1999) Topography of contextual modulations mediated by short-range
762 interactions in primary visual cortex. *Nature* 399:655–661
- 763 Douglas RJ, Martin KAC (2004) NEURONAL CIRCUITS OF THE NEOCORTEX. *Annual*
764 *Review of Neuroscience* 27:419–451
- 765 Douglas RJ, Martin KA, Whitteridge D (1991) An intracellular analysis of the visual responses of
766 neurones in cat visual cortex. *The Journal of Physiology* 440:659–696
- 767 Field DJ, Hayes A, Hess RF (1993) Contour integration by the human visual system: evidence
768 for a local “association field.” *Vision Res* 33:173–193
- 769 Fisker RA, Garey LJ, Powell TP (1975) The intrinsic, association and commissural connections
770 of area 17 on the visual cortex. *Philos Trans R Soc Lond B Biol Sci* 272:487–536
- 771 Geisler WS, Perry JS, Super BJ, Gallogly DP (2001) Edge co-occurrence in natural images
772 predicts contour grouping performance. *Vision Res* 41:711–724
- 773 Gerard-Mercier F, Carelli PV, Pananceau M, et al (2016) Synaptic Correlates of Low-Level
774 Perception in V1. *J Neurosci* 36:3925–3942

- 775 Gilbert CD, Wiesel TN (1979) Morphology and intracortical projections of functionally
776 characterised neurones in the cat visual cortex. *Nature* 280:120–125
- 777 Gilbert CD, Wiesel TN (1989) Columnar specificity of intrinsic horizontal and corticocortical
778 connections in cat visual cortex. *J Neurosci* 9:2432–2442
- 779 Goldberg JA, Rokni U, Sompolinsky H (2004) Patterns of ongoing activity and the functional
780 architecture of the primary visual cortex. *Neuron* 42:489–500
- 781 Grossberg S (1983) The quantized geometry of visual space: The coherent computation of
782 depth, form, and lightness. *Behav Brain Sci* 6:625–657
- 783 Huang X, Elyada YM, Bosking WH, et al (2014) Optogenetic assessment of horizontal
784 interactions in primary visual cortex. *J Neurosci* 34:4976–4990
- 785 Hupé JM, James AC, Payne BR, Lomber SG, Girard P, Bullier J. 1998. Cortical feedback
786 improves discrimination between figure and background by V1, V2 and V3 neurons. *Nature*
787 **394**:784–787. doi:10.1038/29537
- 788 Hunt JJ, Bosking WH, Goodhill GJ (2011) Statistical structure of lateral connections in the
789 primary visual cortex. *Neural Syst Circuits* 1:3
- 790 Jancke D, Chavane F, Naaman S, Grinvald A (2004) Imaging cortical correlates of illusion in
791 early visual cortex. *Nature* 428:423–426
- 792 Jones HE, Grieve KL, Wang W, Sillito AM. 2001. Surround Suppression in Primate V1. *J*
793 *Neurophysiol* 86:2011–2028. doi:10.1152/jn.2001.86.4.2011
- 794 Ju N, Jiang R, Macknik SL, et al (2018) Long-term all-optical interrogation of cortical neurons in
795 awake-behaving nonhuman primates. *PLoS Biol* 16:e2005839
- 796 Kang K, Shelley M, Sompolinsky H (2003) Mexican hats and pinwheels in visual cortex.
797 *Proceedings of the National Academy of Sciences* 100:2848–2853
- 798 Karube F, Kisvárdy ZF (2010) Topographical organization of layer 4 and 6 spiny neurons over
799 functional maps for visual signals in cat area 18. *Neuroscience Research* 68:e152
- 800 Karube F, Sári K, Kisvárdy ZF (2017) Axon topography of layer 6 spiny cells to orientation map
801 in the primary visual cortex of the cat (area 18). *Brain Struct Funct* 222:1401–1426
- 802 Kaschube M, Schnabel M, Lowel S, Coppola DM, White LE, Wolf F. 2010. Universality in the
803 Evolution of Orientation Columns in the Visual Cortex. *Science (New York, NY)* 1–5.
804 doi:10.1126/science.1194869
- 805 Kisvárdy Z (1997) Orientation-specific relationship between populations of excitatory and
806 inhibitory lateral connections in the visual cortex of the cat. *Cerebral Cortex* 7:605–618
- 807 Kisvárdy ZF, Kim DS, Eysel UT, Bonhoeffer T (1994) Relationship between lateral inhibitory
808 connections and the topography of the orientation map in cat visual cortex. *Eur J Neurosci*
809 6:1619–1632
- 810 Koch E, Jin J, Alonso JM, Zaidi Q (2016) Functional implications of orientation maps in primary

- 811 visual cortex. *Nat Commun* 7:1–13
- 812 Laing CR, Troy WC (2003) PDE methods for nonlocal models. *SIAM J Appl Dyn Syst* 2:487–
813 516
- 814 Markov NT, Misery P, Falchier A, et al (2011) Weight consistency specifies regularities of
815 macaque cortical networks. *Cereb Cortex* 21:1254–1272
- 816 Marr D, Hildreth E (1980) Theory of edge detection. *Proc R Soc Lond B Biol Sci* 207:187–217
- 817 Martin KAC, Roth S, Rusch ES (2014) Superficial layer pyramidal cells communicate
818 heterogeneously between multiple functional domains of cat primary visual cortex. *Nat*
819 *Commun* 5:5252
- 820 Martin KAC, Roth S, Rusch ES. 2017. A biological blueprint for the axons of superficial layer
821 pyramidal cells in cat primary visual cortex. *Brain Struct Funct* 222:3407–3430.
- 822 McManus JNJ, Li W, Gilbert CD (2011) Adaptive shape processing in primary visual cortex.
823 *Proc Natl Acad Sci U S A* 108:9739–9746
- 824 Michalski A, Gerstein GL, Czarkowska J, Tarnecki R (1983) Interactions between cat striate
825 cortex neurons. *Exp Brain Res* 51:97–107
- 826 Mitchison G, Crick F (1982) Long axons within the striate cortex: their distribution, orientation,
827 and patterns of connection. *Proc Natl Acad Sci U S A* 79:3661–3665
- 828 Monier C, Chavane F, Baudot P, et al (2003) Orientation and direction selectivity of synaptic
829 inputs in visual cortical neurons: a diversity of combinations produces spike tuning. *Neuron*
830 37:663–680
- 831 Muller L, Chavane F, Reynolds J, Sejnowski TJ (2018) Cortical travelling waves: mechanisms
832 and computational principles. *Nat Rev Neurosci* 19:255–268
- 833 Muller L, Reynaud A, Chavane F, Destexhe A (2014) The stimulus-evoked population response
834 in visual cortex of awake monkey is a propagating wave. *Nat Commun* 5:3675
- 835 Nurminen L, Merlin S, Bijanzadeh M, Federer F, Angelucci A. 2018. Top-down feedback
836 controls spatial summation and response amplitude in primate visual cortex. *Nature*
837 *Communications* 1–13. doi:10.1038/s41467-018-04500-5
- 838 Ozeki H, Finn IM, Schaffer ES, et al (2009) Inhibitory stabilization of the cortical network
839 underlies visual surround suppression. *Neuron* 62:578–592
- 840 Parent P, Zucker SW (1989) Trace inference, curvature consistency, and curve detection. *IEEE*
841 *Transactions on Pattern Analysis and Machine Intelligence* 11:823–839
- 842 Pattadkal JJ, Mato G, van Vreeswijk C, et al (2018) Emergent Orientation Selectivity from
843 Random Networks in Mouse Visual Cortex. *Cell Rep* 24:2042–2050.e6
- 844 Perrinet LU, Masson GS. 2012. Motion-Based Prediction Is Sufficient to Solve the Aperture
845 Problem. *Neural Computation* 24:2726–2750. doi:10.1162/neco_a_00332

- 846 Perrinet LU, Bednar JA (2015) Edge co-occurrences can account for rapid categorization of
847 natural versus animal images. *Sci Rep* 5:11400
- 848 Poort J, Raudies F, Wannig A, Lamme VAF, Neumann H, Roelfsema PR. 2012. The Role of
849 Attention in Figure-Ground Segregation in Areas V1 and V4 of the Visual Cortex. *Neuron*
850 **75**:143–156. doi:10.1016/j.neuron.2012.04.032
- 851
- 852 Raizada RDS, Grossberg S (2003) Towards a theory of the laminar architecture of cerebral
853 cortex: computational clues from the visual system. *Cereb Cortex* 13:100–113
- 854 Rangan AV, Cai D, McLaughlin DW (2005) Modeling the spatiotemporal cortical activity
855 associated with the line-motion illusion in primary visual cortex. *Proc Natl Acad Sci U S A*
856 102:18793–18800
- 857 Rankin J, Avitabile D, Baladron J, et al (2014) Continuation of localized coherent structures in
858 nonlocal neural field equations. *SIAM J Sci Comput* 36:B70–B93
- 859 Rankin J, Chavane F (2017) Neural field model to reconcile structure with function in primary
860 visual cortex. *PLoS Comput Biol* 13:e1005821
- 861 Reynaud A, Masson GS, Chavane F (2012) Dynamics of local input normalization result from
862 balanced short- and long-range intracortical interactions in area V1. *J Neurosci* 32:12558–
863 12569
- 864 Ribot J, Romagnoni A, Milleret C, et al (2016) Pinwheel-dipole configuration in cat early visual
865 cortex. *Neuroimage* 128:63–73
- 866 Roberts M, Delicato LS, Herrero J, Gieselmann MA, Thiele A. 2007. Attention alters spatial
867 integration in macaque V1 in an eccentricity-dependent manner. *Nat Neurosci* 10:1483–
868 1491.
- 869 Rockland KS, Lund JS, Humphrey AL (1982) Anatomical binding of intrinsic connections in
870 striate cortex of tree shrews (*Tupaia glis*). *J Comp Neurol* 209:41–58
- 871 Romagnoni A, Ribot J, Bennequin D, Touboul J (2015) Parsimony, Exhaustivity and Balanced
872 Detection in Neocortex. *PLoS Comput Biol* 11:e1004623
- 873 Rubin DB, Van Hooser SD, Miller KD (2015) The stabilized supralinear network: a unifying
874 circuit motif underlying multi-input integration in sensory cortex. *Neuron* 85:402–417
- 875 Sarti A, Citti G, Petitot J (2008) The symplectic structure of the primary visual cortex. *Biol*
876 *Cybern* 98:33–48
- 877 Schmidt KE, Kim DS, Singer W, et al (1997) Functional specificity of long-range intrinsic and
878 interhemispheric connections in the visual cortex of strabismic cats. *J Neurosci* 17:5480–
879 5492
- 880 Schwarz C, Bolz J (1991) Functional specificity of a long-range horizontal connection in cat
881 visual cortex: a cross-correlation study. *J Neurosci* 11:2995–3007

- 882 Serre T, Oliva A, Poggio T (2007) A feedforward architecture accounts for rapid categorization.
883 Proc Natl Acad Sci U S A 104:6424–6429
- 884 Sigman M, Cecchi GA, Gilbert CD, Magnasco MO (2001) On a common circle: natural scenes
885 and Gestalt rules. Proc Natl Acad Sci U S A 98:1935–1940
- 886 Sillito AM, Grieve KL, Jones HE, et al (1995) Visual cortical mechanisms detecting focal
887 orientation discontinuities. Nature 378:492–496
- 888 Somers DC, Nelson SB, Sur M (1995) An Emergent Model of Visual Cortical Orientation
889 Selectivity in cat visual cortical simple cells. The Journal of Neuroscience 15:5448–5465
- 890 Ts'o DY, Gilbert CD, Wiesel TN (1986) Relationships between horizontal interactions and
891 functional architecture in cat striate cortex as revealed by cross-correlation analysis. J
892 Neurosci 6:1160–1170
- 893 Tsodyks MV, Skaggs WE, Sejnowski TJ, McNaughton BL (1997) Paradoxical effects of external
894 modulation of inhibitory interneurons. J Neurosci 17:4382–4388
- 895 Vidyasagar TR, Eysel UT. 2015. Origins of feature selectivities and maps in the mammalian
896 primary visual cortex. *Trends in Neurosciences* 38:475–485. doi:10.1016/j.tins.2015.06.003
- 897 Villette V, Chavarha M, Dimov IK, et al (2019) Ultrafast Two-Photon Imaging of a High-Gain
898 Voltage Indicator in Awake Behaving Mice. Cell 179:1590–1608.e23
- 899 Voges N, Guijarro C, Aertsen A, Rotter S (2010) Models of cortical networks with long-range
900 patchy projections. J Comput Neurosci 28:137–154
- 901 Voges N, Perrinet L (2012) Complex dynamics in recurrent cortical networks based on spatially
902 realistic connectivities. Front Comput Neurosci 6:
- 903 Walker EY, Sinz FH, Cobos E, et al (2019) Inception loops discover what excites neurons most
904 using deep predictive models. Nat Neurosci 22:2060–2065
- 905 Wertheimer M (1923) Untersuchungen zur Lehre von der Gestalt. II. Psychologische Forschung
906 4:301–350
- 907 Yousef T, Bonhoeffer T, Kim DS, et al (1999) Orientation topography of layer 4 lateral networks
908 revealed by optical imaging in cat visual cortex (area 18). Eur J Neurosci 11:4291–4308
- 909 Yousef T, Tóth E, Rausch M, et al (2001) Topography of orientation centre connections in the
910 primary visual cortex of the cat. Neuroreport 12:1693–1699
- 911 Zhang Z, Russell LE, Packer AM, et al (2018) Closed-loop all-optical interrogation of neural
912 circuits in vivo. Nat Methods 15:1037–1040
- 913